atmosphere

Article

Convection-Permitting Future Climate Simulations for Bulgaria under the RCP8.5 Scenario

Rilka Valcheva *, Ivan Popov and Nikola Gerganov

National Institute of Meteorology and Hydrology, 1784 Sofia, Bulgaria; ivan.popov@meteo.bg (I.P.); nikola.gerganov@meteo.bg (N.G.)
* Correspondence: rilka.valcheva@meteo.bg

Abstract: In recent decades, climate change has become a critical global issue with far-reaching consequences for regional climates and ecosystems. While regional climate models provide valuable information, there is a growing need for high-resolution simulations to assess local impacts. This paper addresses this gap by presenting the first simulation of a 3 km convection-permitting (CP) scenario simulation for Bulgaria. The main aim of this study is to assess different precipitation indices and their future changes for Bulgaria under the Representative Concentration Pathway 8.5 (RCP8.5) scenario following the Coordinated Regional Climate Downscaling Experiment Flagship Pilot Study protocol. The simulations are evaluated against high-resolution observations. We downscale Coupled Model Intercomparison Project 5 Global Climate Model (CMIP5 GCM) data for historical (1995–2004) and future (2089–2098) periods using a regional climate model (RCM) at 15 km grid spacing and parametrized convection. We use these fields as initial and boundary conditions for convection-permitting kilometer-scale simulations. The 15 km grid spacing driving model is used as a reference to assess the added value of the kilometer-scale simulation. Additionally, the 3 km seasonal mean and projected 2 m temperature and the winter snow water equivalent are presented. The results show that the kilometer-scale simulation shows better performance of wet-hour intensity in all seasons, wet-hour frequency in the spring, fall, and winter, and extreme precipitation (99.9th percentile of all precipitation events, p99.9) in the winter and fall. The kilometer-scale simulation improves the projected precipitation distribution and modifies the signal of the precipitation frequency, intensity, and heavy precipitation change over some areas. A positive projected change in the wet-hour intensity is expected in all seasons (13.86% in spring, MAM, 17.48% in summer, JJA, 1.97% in fall, SON, and 17.43% in winter, DJF) and in the heavy precipitation in the spring (13.14%) and winter (31.19%) in the kilometer-scale experiment. The projected increase in mean winter precipitation is accompanied by a significant decrease in mean winter snowfall over lowlands (50−70%). The convection-permitting Regional Climate Model, version 4.7.1 (RegCM4.7.1) suggests an increase in winter snowfall over the highest parts of the country, but a significant increase in the 2 m temperatures there. The results of this study are encouraging and may be of interest to the community of climate scientists and users of climate data for making reliable estimates of the local impacts of future climate change.

Keywords: convection-permitting modeling; regional climate modeling; climate projections; extreme precipitation; frequency; intensity; kilometer-scale; Bulgaria

check for updates

Citation: Valcheva, R.; Popov, I.; Gerganov, N. Convection-Permitting Future Climate Simulations for Bulgaria under the RCP8.5 Scenario. *Atmosphere* **2024**, *15*, 91. https://doi.org/10.3390/atmos15010091

Academic Editor: Nicola Scafetta

Received: 21 November 2023
Revised: 6 January 2024
Accepted: 8 January 2024
Published: 10 January 2024

1. Introduction

Recent advances in supercomputer power and the development of regional climate models (RCMs) provide the opportunity to run regional climate models at a kilometer-scale resolution [1–6]. These models represent convection explicitly without a convection parametrization scheme and are commonly called "convection-permitting" models (CPMs) [1–3,6,7]. Regional climate models use a convection parametrization scheme, and they have typical grid spacing greater than 10 km. Such convection schemes are known as the main source of model errors and uncertainties [5–9]. Convection-permitting regional climate models (CPRCMs) appeared as a hopeful tool to improve the representation of precipitation metrics at the hourly and sub-daily timescales [7,9]. An increase in computational resources has made it possible to run regional climate models on kilometer-scale grid spacing even at continental domains. Several international projects have been launched to produce and compare convection−permitting climate simulations from different climate research institutes and universities in Europe (the Coordinated Regional Climate Downscaling Experiment Flagship Pilot Studies, CORDEX-FPS [1], the European Climate Prediction System, EUCP [10]). Recent studies using 10-year-long convection-permitting simulations reveal that finer resolution reduces the present-day biases in precipitation [11,12]. The results in [12] confirm the improved performance of CP models in simulating important characteristics of daily and hourly precipitation and extreme events. CPMs show improvements in the spatial structure and diurnal cycle of precipitation [6,7,9,13,14]. Recently, the first ensemble CP multi-model assessment studies were performed over the domain of the Mediterranean and the Alps region [1,11]. The advantages of convection-permitting models concerning regional climate models are evident, especially for sub-daily precipitation [4,15,16], and precipitation frequency and intensity are better represented over complex terrain with kilometer-scale models [9,17,18].

Climate change simulations at the CP scale are now available for continental domains. For example, CP continental simulations for Europe are shown in [19–21], and those for Africa and North America are shown in [22,23]. Pichelli [24] presents the first multi-model ensemble of 10-year CP scenario simulation over the Alpine region. The main findings confirm that the kilometer-scale ensemble can improve the representation of mean daily and hourly precipitation metrics and modify the precipitation change signal over some regions. Chan [19] examines the km-scale projected changes for a European-wide domain using the 2.2 km UK, Exeter Met Office Unified Model. Unfortunately, the territory of Bulgaria, as a county in southeastern Europe, is not considered in these studies. Lucas−Picher [3] gives an overview of the latest developments using convection-permitting regional climate models. Recent studies show enhanced changes in extreme precipitation over Europe compared with regional climate models [19,24,25]. Collaborations among several institutes have performed multi-model-based convection-permitting simulations (CORDEX-FPS). Coppola [1] examines climate sensitivity studies of different CP models and their uncertainties. However, it should be noted that high-resolution models with grid spacings on a km scale still apply parameterizations for microphysics, turbulence, and shallow convection. High spatial-resolution climate simulations need high-resolution gridded observational datasets for evaluation [26]. This problem becomes especially relevant for regions with sparsely distributed weather stations.

The regional climate model version 4 (RegCM4) [2,27] was used in this study. The model has a non-hydrostatic dynamic core based on MM5, which can be used for km-scale applications [2]. The present-day/hour performance of the RegCM4 model for Bulgaria was recently investigated in [28–30] for the period 2000–2010 using ERA-Interim as an initial and boundary condition. The aim of this study is to assess historical (1995–2004) and future (2089–2098) climate simulations with the RegCM version 4.7.1 model at regional and convection-permitting scales for Bulgaria. The special focus is on precipitation metrics and also on future 2 m temperature and winter snowfall. This is the first time that CPM has been used to provide Bulgarian future climate projections at the km-scale. These new simulations allow us to examine the benefits of CPMs across the county. The novel aspects of this study are connected with producing very high spatial and temporal resolution climate change information for this region that will be of interest to climate information users, such as policymakers, stakeholders, and others, for the assessment of the added value of CPM simulation regarding RCM simulation and the assessment of the impact of climate change on heavy precipitation events, winter snowfall, and 2 m temperature for Bulgaria. The periods were chosen following the CORDEX−FPS protocol [1].

This paper is structured as follows: In Section 2, we present the materials and methods used in this study. Section 3 provides an assessment of precipitation metrics at daily and hourly scales for the historical period and also the future climate projections of precipitation indices, winter snowfall, and 2 m temperature for the territory of Bulgaria. In Section 4, we present a discussion and the conclusions.

2. Materials and Methods

2.1. Study Area

Bulgaria is situated in southeastern Europe on the Balkan Peninsula (Figure 1). It is known for its diverse geography, which includes mountains, plains, and a coastline along the Black Sea. Located in southwestern Bulgaria, the Rila Mountain is home to the highest peak in the Balkan Peninsula, Musala, which reaches an elevation of 2925 m. The country experiences a wide range of precipitation patterns, influenced by both continental and Mediterranean climate regimes, as well as local topographic features such as mountains, valleys, and coastal areas [31]. Precipitation plays a crucial role in the water balance and ecosystems of Bulgaria. This makes the accurate simulation of historical and future precipitation statistics of paramount importance for various sectors like agriculture, hydrology, and disaster risk management. The simulations were performed on a Discoverer supercomputer located in Sofia (Bulgaria), with a time-stepping of 6 s and a model domain of 260 × 200 grid points for the CP simulations. The forcing at the lateral boundaries was updated every 6 h.

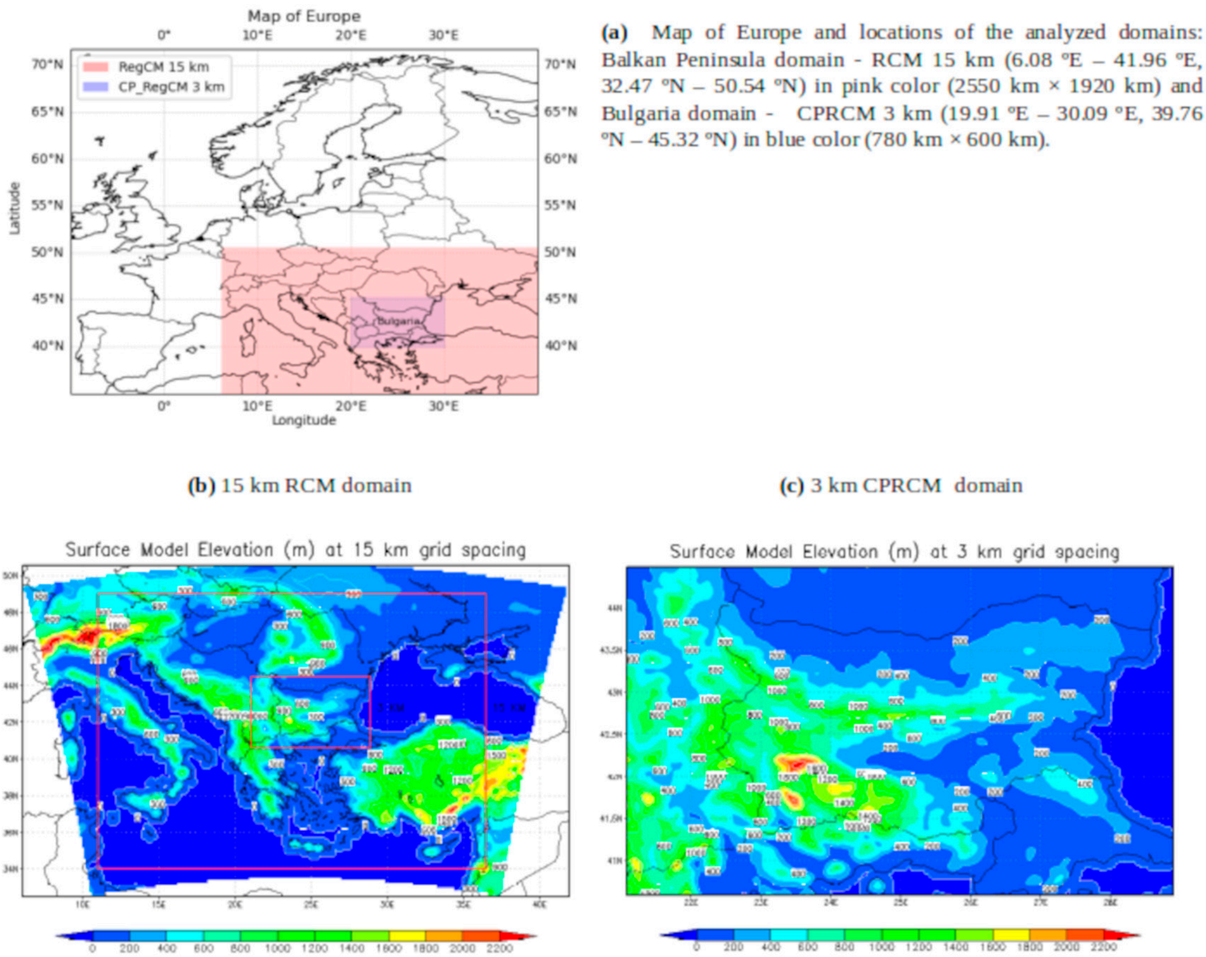

Figure 1. Analyzed domains (**a**) and surface model elevation (m) at a 15 km grid spacing for the Balkan Peninsula domain (**b**) and a 3 km grid spacing for Bulgaria (**c**). The red line indicates the analyzed domains after removing the buffer zone from each size.

2.2. The RegCM Model

In this study, historical and future 10-year simulations at 15 km (RCM) and 3 km (CPRCM) grid spacings were performed with the RegCM4 [2,27] model. It uses the CCSM radiation scheme [32]; the planetary boundary layer is parametrized with a modified Holtslag scheme [33], and the microphysics scheme is SUBEX [34]. For land surface representation, we used the BATS scheme [35], and for ocean fluxes, we followed Zeng [36]. The Kain–Fritsch cumulus convection scheme was used [37,38] for the intermediate simulation, and the MM5 shallow cumulus scheme [2,39] was used for the convection-permitting (CP) simulations. This configuration was chosen in previous studies [28,29,40] and showed the best results for the studied territory. We use a Lambert Conformal Conic projection suitable for mid-latitudes. For the initial and lateral boundary conditions for the intermediate run, the CMIP5 GCM HadGEM2−ES (Met Office Hadley Centre Global Climate Model) [41] under the RCP8.5 scenario [42] was used for the periods 1975–2004 and 2089–2098 and updated every 6 h for the Balkan Peninsula region. It provides data for the initial and lateral boundary conditions for the convection-permitting run at a 3 km grid spacing. This business-as-usual scenario represents the worst-case future, in which no climate change mitigation measures are taken. The HadGEM2−ES global climate model has 38 vertical levels (~40 km height) and horizontal grid spacings of 1.25° × 1.875°. This is equivalent to a grid spacing of about 120 km × 139 km at mid-latitude.

2.3. Simulation Set-Up

The CP simulation (260 × 200 grid cells) has a horizontal grid spacing of 3 km, 41 vertical levels, and a time step of 6 s. The CP model (CPRCM) is nested into the regional climate model (RCM) (170 × 128 grid cells) at a 15 km grid spacing driven by the HadGEM2−ES GCM [41] (1.25° × 1.875°) (Figure 1). Both models use the non-hydrostatic dynamical core of RegCM. For coarse-resolution simulation, we used parameterized deep convection, while for the km-scale simulation, we used only shallow convection. The simulations were evaluated against high-resolution data. Both simulations used the years 1994 and 2088 as a spin-up, and these years were removed from the analysis.

The CP simulation ran on the Bulgarian European High Performance Computing Joint Undertaking (EuroHPC JU) Discoverer supercomputer using, on average, 500 processors, for a total actual runtime of about 1400 h (0.7 million core-hours) and 20 TB of disk usage before post-processing for its 20 years of 3 km simulations. The analysis of the 3 km and 15 km simulations is presented in Section 3.

2.4. Data Sources

The availability of high-resolution and quality datasets is a key issue when assessing CP-scale simulation. For the assessment of daily precipitation metrics, we used MESCAN_SURFEX re-analyses at 5.5 km resolution [43,44] and the PERSIANN Dynamic Infrared–Rain Rate (PERSIANN-PDIR-Now) satellite data at a 0.04-degree resolution [45] for daily/hourly precipitation evaluation (Table 1).

Table 1. Observational datasets.

Name/Availability	Spatial Resolution	Temporal Resolution	Data Source and Region	References
MESCAN−SURFEX (1961–2019)	5.5 × 5.5 km	daily	Surface re-analysis (Europe)	[43,44]
PERSIANN−PDIR−Now (March 2000–now)	0.04° × 0.04°	hourly/daily	Satellite (global)	[45]

Uncertainties connected with different types of sensors for precipitation measurements are discussed in [46–49] and should be considered. For example, for in situ precipitation data, errors are usually connected with low station density, especially over higher elevations, and precipitation intensities are often underestimated in windy conditions.

2.5. Statistical Indices

In this study we use several precipitation indices (Table 2) to assess the performance of regional and CP simulations: daily mean precipitation, daily and hourly precipitation intensity and frequency, and heavy precipitation (p99/p99.9) defined as the 99th and 99.9th percentiles of all precipitation events, respectively (Table 2). For daily and hourly precipitation intensity and frequency, we use wet days/hours with precipitation greater than 1 mm/0.1 mm, respectively. For daily and hourly extreme precipitation (p99 and p99.9, respectively), we use all precipitation events (wet and dry) [50]. The indices are calculated for the summer (JJA), spring (MAM), fall (SON), and winter (DJF) seasons. For the evaluation of the km-scale simulation, the observational data are interpolated on a 3 km grid using the distance-weighted interpolation method and on a 15 km grid for the assessment of coarse-resolution simulation.

Table 2. Daily and hourly precipitation indices.

Indicators	Description	Units
Mean precipitation	Daily mean precipitation.	mm/d
Frequency	Wet day and hour frequency is defined as a % of the number of wet days/hours per season.	(%)
Intensity	Wet day and wet hour intensity.	mm/d; mm/h
Heavy precipitation	Defined as the 99th percentile of all daily precipitation events (p99) and the 99.9th percentile of all hourly precipitation events (p99.9).	mm/d; mm/h
Bias	Model—observation.	mm/d; mm/h; (%)
PDF	Probability density function of hourly/daily precipitation	

3. Results

Even though convective events in Bulgaria are predominant in the spring and summer, our assessment focuses on all seasons (MAM, JJA, SON, and DJF) and shows spatial maps of the means and biases for all indices. This is because no previous studies using convection-permitting regional climate projections have been reported for Bulgaria.

3.1. Historical Climate Simulations, 1995−2004

3.1.1. Hourly Precipitation Metrics, 2001−2004

Figures 2–4 show the spatial distribution of seasonal means and biases of wet hour intensity, frequency, and extreme precipitation (p99.9) for all seasons, respectively. The first column of each figure represents the seasonal means of high-resolution observational data, the second and third show km-scale and coarse-resolution means, respectively, while the last two columns show the mean biases of the CP and RCM simulations concerning the observational data. The km-scale simulation generally better represents the precipitation indices at the hourly scale in all seasons, especially for wet-hour intensity, improving the spatial distribution of the coarse-resolution simulation. With an increase in resolution, an increase in details is noticeable, which is related to a more precise representation of the topography and the subsequent interactions between the orography and dynamical processes.

Figure 2 shows the seasonal mean wet-hour precipitation intensity (more than 0.1 mm/h) depicted with PDIR−Now and simulated with 15 km RCM and 3 km CPRCM (first three columns) and the mean biases of both models with regard to the PDIR observational data (last two columns). Both models have similar biases in the fall and winter of being too dry. CPRCM corrected the fall intensity in central Bulgaria. In the spring and summer, both models have different performances, with CPRCM being too wet in the summer and in the westernmost part of Bulgaria in the spring and RCM being too dry (~40%, not shown here). The RCM underestimation of wet-hour intensity is overall corrected with CPRCM in the seasons when convective precipitation occurs (MAM, JJA, SON). The area-averaged means and biases concerning the high-resolution observation are reported in Table 3. Compared with the PDIR−Now data, improvements were found in the km-scale simulation for wet-hour intensity in all seasons compared with the coarse-resolution simulation (−12% vs. −36.8% in the spring; +3.7% vs. −41.4% in the summer; −44.5% vs. −53.7% in the fall; −47.6% vs. −57.9% in the winter).

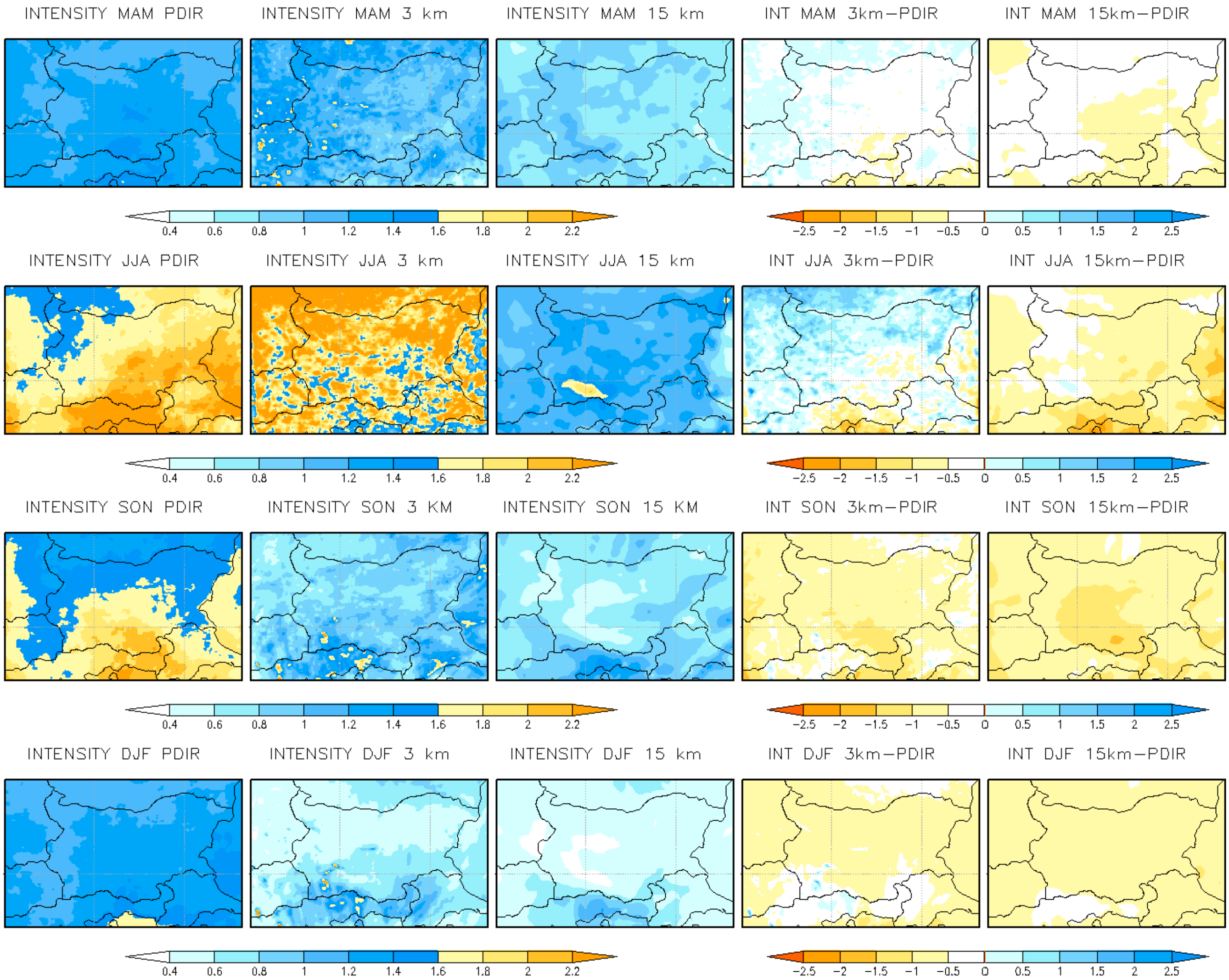

Figure 2. Spatial distribution of seasonal mean wet-hour intensity (>0.1 mm/h) from observations (PDIR−Now) and simulations (3 km CPRCM and 15 km RCM) (first three columns) and mean biases of CPRCM and RCM concerning PDIR_Now (last two columns) for MAM (first row), JJA (second row), SON (third row), and the winter (last row). The simulated period is 2001−2004.

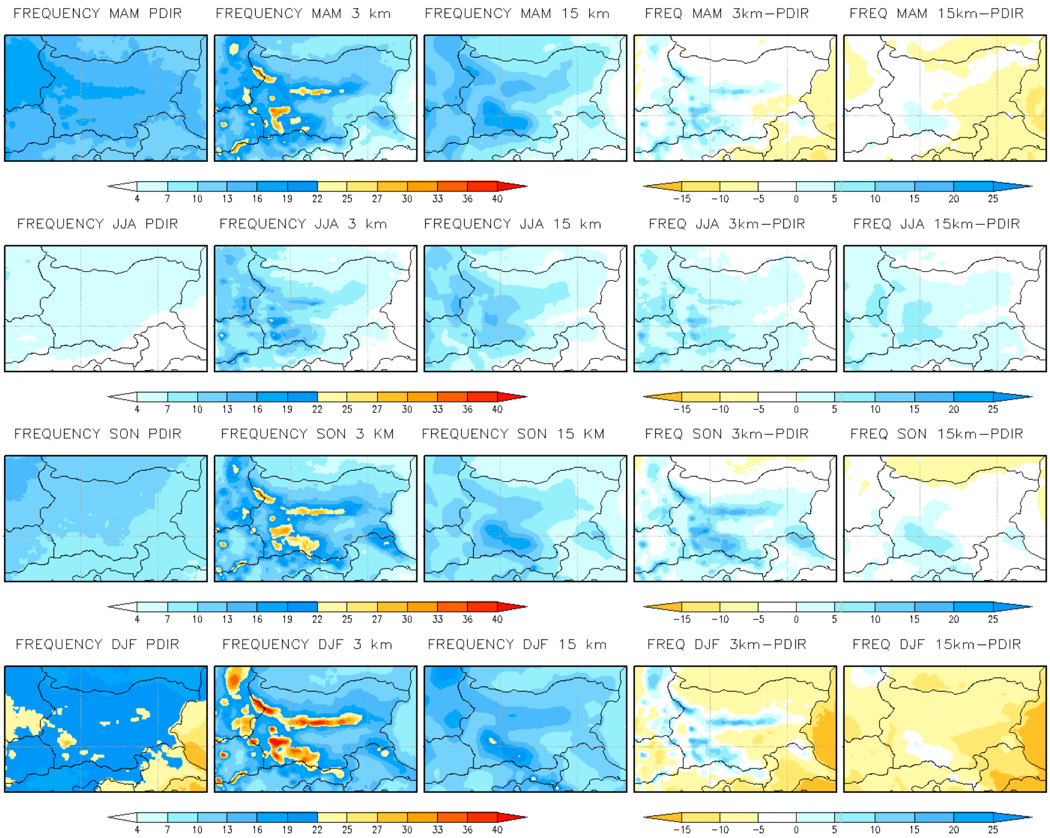

Figure 3. Same as Figure 2, but for wet-hour frequency (>0.1 mm/h) in %.

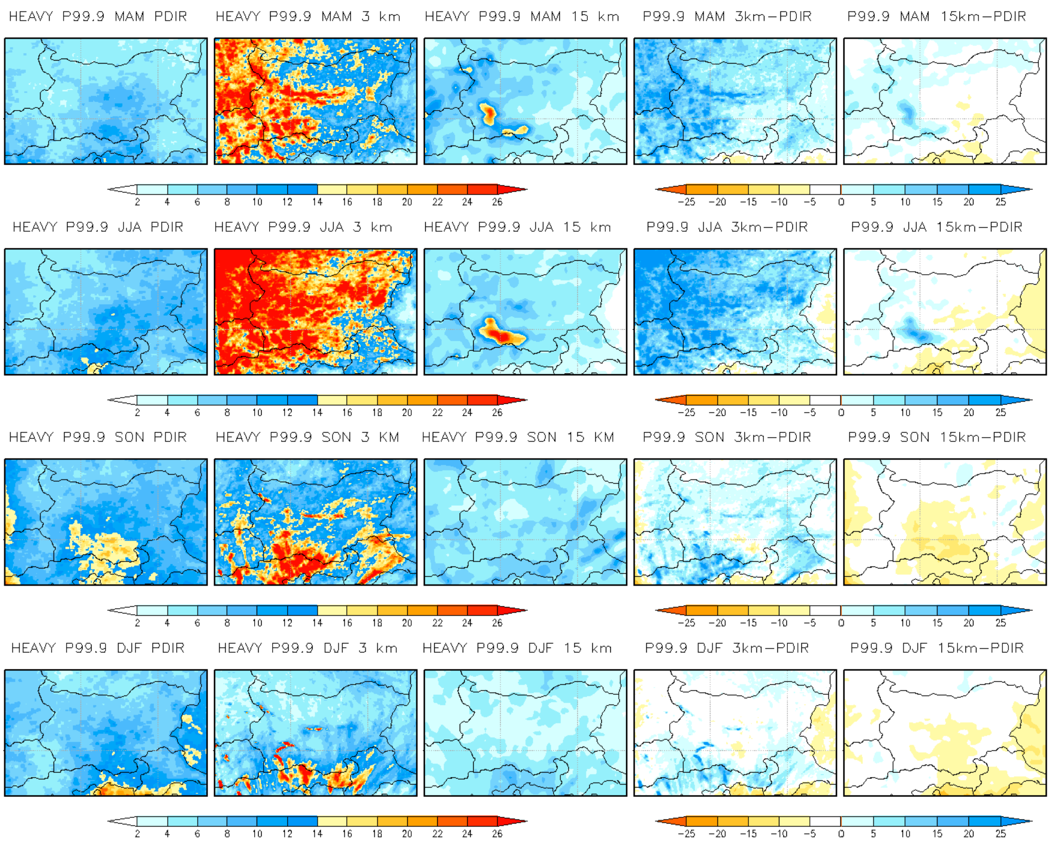

Figure 4. Same as Figure 2, but for heavy hourly precipitation p99.9 in mm/h.

Table 3. Seasonal means and mean biases for the daily (mm/d) and hourly (mm/h) analyzed indices (except frequency in %) from observations and simulations area-averaged for Bulgaria over the historical period 1995–2004. The historical period for hourly precipitation is 2001–2004. The OBS refers to the PDIR-Now dataset for hourly precipitation metrics and to the MESCAN-SURFEX dataset for daily precipitation metrics.

Historical Period	OBS	CPRCM 3 km	RCM 15 km	RCM 15 km—OBS	CPRCM 3 km—OBS
MAM—hourly					
INT	1.25	1.1	0.79	−0.46	**−0.15**
FREQ	14.49	12.49	9.47	−5	**−2**
P99.9	6.43	14.75	5.66	−0.79	8.33
MAM—daily					
Mean PR	1.99	3.31	1.75	−0.23	1.32
INT	6.2	8.74	5.37	−0.83	2.54
FREQ	30.27	35.02	29.69	−0.49	4.75
P99	21.6	40.67	19.21	−2.37	19.07
JJA—hourly					
INT	1.91	1.98	1.12	−0.79	**0.07**
FREQ	5.14	7.02	6.42	1.29	1.88
P99.9	7.94	20.12	5.26	−2.68	12.18
JJA—daily					
Mean PR	2.11	3.39	1.78	−0.32	1.28
INT	6.71	11.71	5.79	−0.92	5
FREQ	29.29	26.25	27.95	−1.22	−3.04
P99	22.66	49.89	20.03	−2.58	27.24
SON—hourly					
INT	1.64	0.92	0.77	−0.88	**−0.73**
FREQ	10.39	12.29	8.43	−1.97	**1.89**
P99.9	10.09	12.3	5.5	−4.61	**2.21**
SON—daily					
Mean PR	1.91	2.93	1.76	−0.15	1.02
INT	7.78	9.03	6.73	−1.1	1.25
FREQ	23.69	30.67	24.39	0.7	6.98
P99	25.49	44.05	24.19	−1.34	18.55
DJF—hourly					
INT	1.26	0.66	0.53	−0.73	**−0.6**
FREQ	21.34	15.61	11.97	−9.39	**−5.74**
P99.9	8.61	7.69	4.31	−4.33	**−0.93**
DJF—daily					
Mean PR	1.72	2.54	1.63	−0.1	0.82
INT	6.38	7.1	5.06	−1.32	**0.72**
FREQ	25.51	33.56	29.79	4.25	8.05
P99	21.27	30.85	18.42	−2.84	9.58

Figure 3 shows the wet-hour frequency (above 0.1 mm/h) means from the simulations and observations and mean biases of RCM and CPRCM for the PDIR datasets for all seasons. Wet-hour frequency is improved when using CPRCM compared with RCM (Figure 3), especially for MAM (−2% vs. −5%), SON (+1.89% vs. −1.97%), and DJF (−5.74% vs. −9.39%) (Table 3). However, the km-scale simulation overestimates wet-hour frequency over the topography (Figure 3, fourth column) in all seasons, especially in the winter and fall. In the spring and winter, RCM underestimates wet-hour frequency (Figure 3, last column), especially over eastern and southeastern parts of Bulgaria by about 10−15%. In summer and fall, RCM underestimates the wet-hour intensity (Figure 2, last column in the middle) and overestimates the frequency (Figure 3, last column in the middle). This is a well-known issue in regional climate models producing weak and frequent precipitation, the so-called 'drizzle problem', which is generally improved with km-scale simulations [7,24]. This behavior is particularly corrected with CPRCM, especially in the fall for Bulgaria.

Figure 4 shows the spatial distribution of extreme precipitation for Bulgaria defined as the 99.9th percentile of all precipitation events for all seasons and mean biases (last two columns) with regard to PDIR observational data. Overall, RCM underestimates p99.9 in all seasons, except for the mountains in the summer and spring. The RCM underestimation in the fall and winter is generally corrected with CPRCM. We found improvements in p99.9 representation in the kilometer-scale simulation for the autumn (+21.9% vs. −45.7%) and winter (−10.8% vs. −50.3%). However, CPRCM significantly overestimates the spring and summer extreme precipitation (p99.9) (above 100%). Table 3 presents area-averaged means and biases for the territory of Bulgaria over the historical periods 1995–2004 (for daily precipitation metrics) and 2001–2004 (for hourly precipitation metrics). The km-scale improvements are marked in bold in Table 3.

The area-average biases for the territory of Bulgaria show that the km-scale simulation presents better results compared with the coarse-resolution simulation for wet-hour intensity in all seasons (−12% vs. −36.8% in the spring; +3.7% vs. −41.4% in the summer; −44.5% vs. −53.7% in the fall; −47.6% vs. −57.9% in the winter). Improvements were found in wet-hour frequency biases in MAM (−2% vs. −5%) and DJF (−5.74% vs. −9.39%) when compared with the CPRCM and RCM simulations, respectively. The kilometer-scale simulation better represents heavy precipitation (p99.9) for Bulgaria in SON (+21.9% vs. −45.7%) and DJF (−10.8% vs. −50.3%) compared with the 15 km coarse-resolution simulation. These results confirm the improvements found in a previous study [28] for the territory of Bulgaria, showing an assessment of present-day/hour kilometer scale simulation for Bulgaria with ERA-Interim boundary conditions for a 10-year-long period (2000–2010).

The probability density functions (PDFs) for hourly (Figure 5) and daily (Figure S7) precipitation are also presented for Bulgaria. Figure 5 reports the historical PDIR-Now-observed distribution (2001–2004), RCM and CPRCM (1995–2004), and the future RCM and CPRCM (2089–2098) distributions. In this order, the colors are dark blue, dark brown, bright brown, green, and bright blue. Referring to the historical period, the high-resolution distribution of the PDIR-Now observational dataset (dark blue) shows a tail reaching 70 mm/h for hourly precipitation (Figure 5, dark blue) and 150 mm/d for daily precipitation (Figure S7, yellow). The MESCAN-SURFEX distribution shows 120 mm/d (Figure S7, dark blue). The PDFs for hourly precipitation show an overestimation with the driving RCM (dark brown) and an overestimation with the CPRCM (bright brown). CPRCM shows greater overestimation than RCM. The longer tail of CPRCM indicates an overestimation of the most extreme precipitation. The PDFs for daily precipitation also show an overestimation of the RCM and CPRCM of extreme precipitation and differences between the observed distributions (PDIR-Now overestimates the MESCAN_SURFEX most extreme precipitation). For the future period, the PDFs for the daily (Figure S7) and hourly (Figure 5) distributions show a positive change in heavy hourly and daily precipitation for Bulgaria.

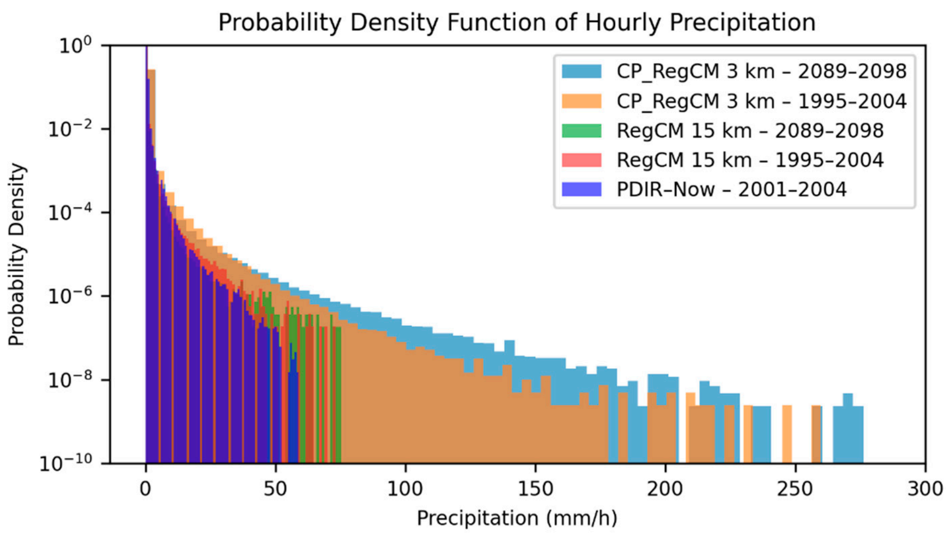

Figure 5. Probability density function (PDF) for hourly precipitation for Bulgaria from simulations and observation for the historical (1995–2004) and future (2089–2098) periods. The PDIR-Now dataset is available for the period 2001–2004. Dark blue is used for the PDIR-Now dataset. Light blue is used for the CPRCM future and bright brown for historical periods. Green is used for the coarse RCM historical (1995–2004), and dark brown is used for the future (2089–2098) periods.

3.1.2. Daily Precipitation Metrics for the Historical Period of 1995–2004

Figures S1–S4 in the Supplementary Materials present results for the seasonal mean daily precipitation metrics: mean daily precipitation, wet day intensity, frequency, and heavy precipitation (p99) for the historical period (1995–2004). Although the kilometer-scale simulation overestimates mean daily precipitation in all seasons, especially over topography, it reproduces the precipitation distribution over Bulgaria more realistically than the coarse-resolution simulation (Figure S1). Figure S1 shows the spatial distribution of the seasonal mean daily precipitation (mm/d) from observations (MESCAN−SURFEX) and simulations (3 km and 15 km simulations) (first three columns) and mean biases of CPRCM and RCM concerning MESCAN (last two columns) for the spring (first row), summer (second row), autumn (third row) and winter (last row). The simulated historical period is 1995−2004. The km-scale simulation overestimates the mean daily precipitation in all seasons (+66.3% in MAM; +60.7% in JJA; +53.4% in SON, and +47.7% in DJF), especially over topography (Figure S1, fourth column), while RCM underestimates it in JJA (except for the mountains) and in MAM and SON over eastern and northeastern Bulgaria (Figure S1, last column). CPRCM overestimates the wet-day intensity in all seasons (+41% in MAM; +74.5% in JJA; +16.1% in SON, and +11.3% in DJF), especially in JJA and MAM, and in SON and DJF over topography (Figure S2, fourth column). RCM underestimates wet-day intensity in all seasons, except for the mountains in the summer and spring and the westernmost parts of Bulgaria in MAM (Figure S2, last column). CPRCM overestimates the wet-day frequency in the spring, fall, and winter (+4.75% in MAM; +6.98% in SON; +8.05% in DJF), especially over the mountains. In the summer, CPRCM overestimates frequency over topography and underestimates it in eastern Bulgaria (Figure S3, fourth column). The results with RCM in the summer are similar. RCM overestimates precipitation the wet-day frequency over the mountains in all seasons and underestimates it over eastern Bulgaria in the spring and summer (Figure S3, last column). The kilometer-scale simulation shows a large overestimation of extreme precipitation (p99) in all seasons (89.7% in MAM; 126% in JJA; 81.9%% in SON, and 37.6% in DJF) (Figure S4, fourth column), while the coarse-resolution simulation underestimates extreme precipitation (p99) in all seasons, except for the mountains (Figure S4, last column).

Figures S5 and S6 show an additional evaluation of the daily precipitation indices with respect to the daily PDIR-Now dataset. Figure S5 shows the spatial distribution of the seasonal mean biases of CPRCM for mean precipitation, intensity, frequency, and p99. Figure S6 shows the same values as Figure S5 but for the intermediate RCM simulation. CPRCM overestimates mean daily rainfall, wet-day intensity, and heavy precipitation (p99) in all seasons, especially in the summer and spring, and underestimates the wet-day frequency in all seasons, except in the summer over the mountains. On the other hand, RCM (Figure S6) underestimates the mean daily precipitation and heavy precipitation in the fall and winter and p99 in the spring and summer over southeastern Bulgaria. RCM overestimates the mean daily precipitation, intensity, and p99 in the spring and underestimates frequency in all seasons, except for western Bulgaria in the summer.

3.2. Future Climate Simulations 2089−2098 vs. 1995–2004

3.2.1. Hourly Projection Precipitation Change in 2089−2098 vs. 1995–2004

Figure 6 compares the expected changes (%) in wet-hour intensity, wet-hour frequency, and heavy precipitation (p99.9) from both models (3 km and 15 km simulations) related to the spring (first two columns) and summer (last two columns) by the end of the century. Figure 7 shows the same values as Figure 6 but for the autumn and winter change in %.

The climate projections for precipitation are similar between resolutions. Simulated area-averaged projected changes (%) for the end of the century 2089–2098 concerning the historical period 1995–2004 from both simulations are presented in Table 4. CPRCM and RCM present similar results, but the kilometer-scale simulation shows more intense heavy precipitation (p99.9) in the spring and winter and less frequent events in the summer. When comparing both resolutions, the wet-hour intensity from CPRCM and RCM is expected to increase in all seasons (+13.86% vs. +18.11% in MAM; +17.48% vs. +9.76% in JJA; +1.97% vs. +5.2% in SON, and +17.43% vs. +18.44% in DJF) (Figures 6 and 7), respectively, except the northeastern part of Bulgaria in the fall (Figure 7, first row). The wet-hour frequency is expected to decrease in all seasons according to CPRCM and RCM (−1.75% vs. −1.21% in MAM; −2.99% vs. −2.65% in JJA; −2.26% vs. 2.14% in SON), respectively, except for the 3 km winter simulation (+0.54% vs. −0.19% in DJF) (Figure 7, second row). The area-average changes for Bulgaria show that heavy precipitation (p99.9) is expected to increase in DJF and MAM and decrease in JJA and SON according to the 3 km and 15 km simulations (+13.14% vs. +8.71% in MAM; −15.52% vs. −4.88% in JJA; −0.14% vs. −0.86% in SON; +31.19% vs. +25.66% in DJF), respectively, except for the autumn simulation over the central and north-westernmost parts of the country (Figure 7, last row), where the CP simulation shows a 30% increase in heavy precipitation (p99.9). On the contrary, RCM shows a significant decrease in p99.9 in the spring over the western part of the country (Figure 6).

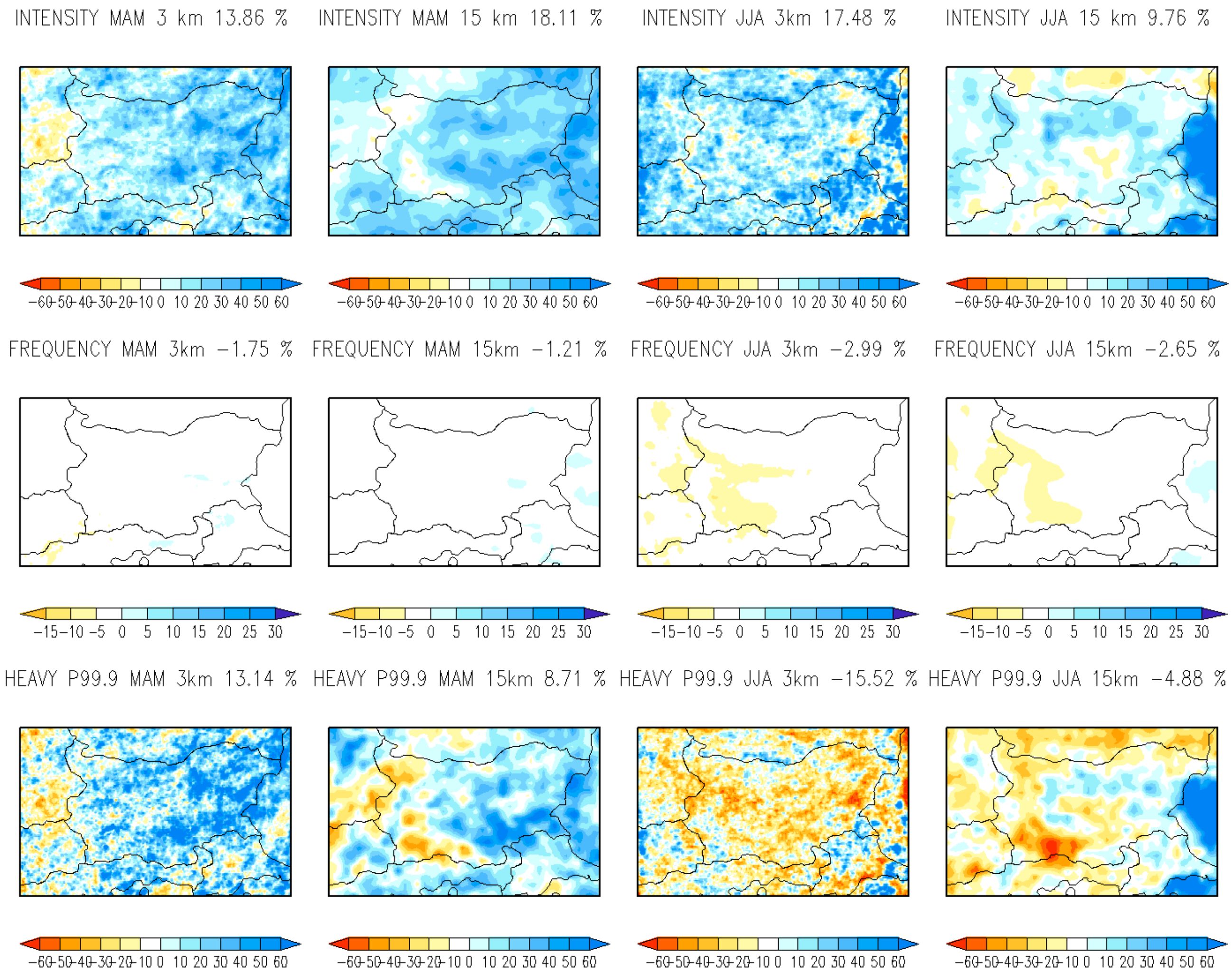

Figure 6. Expected changes in hourly intensity (first row), frequency (middle row), and heavy precipitation (p99.9) (last row) from both models (3 km CPRCM and 15 km RCM) related to the spring (first two columns, respectively) and summer (last two columns, respectively) by the end of the century in %.

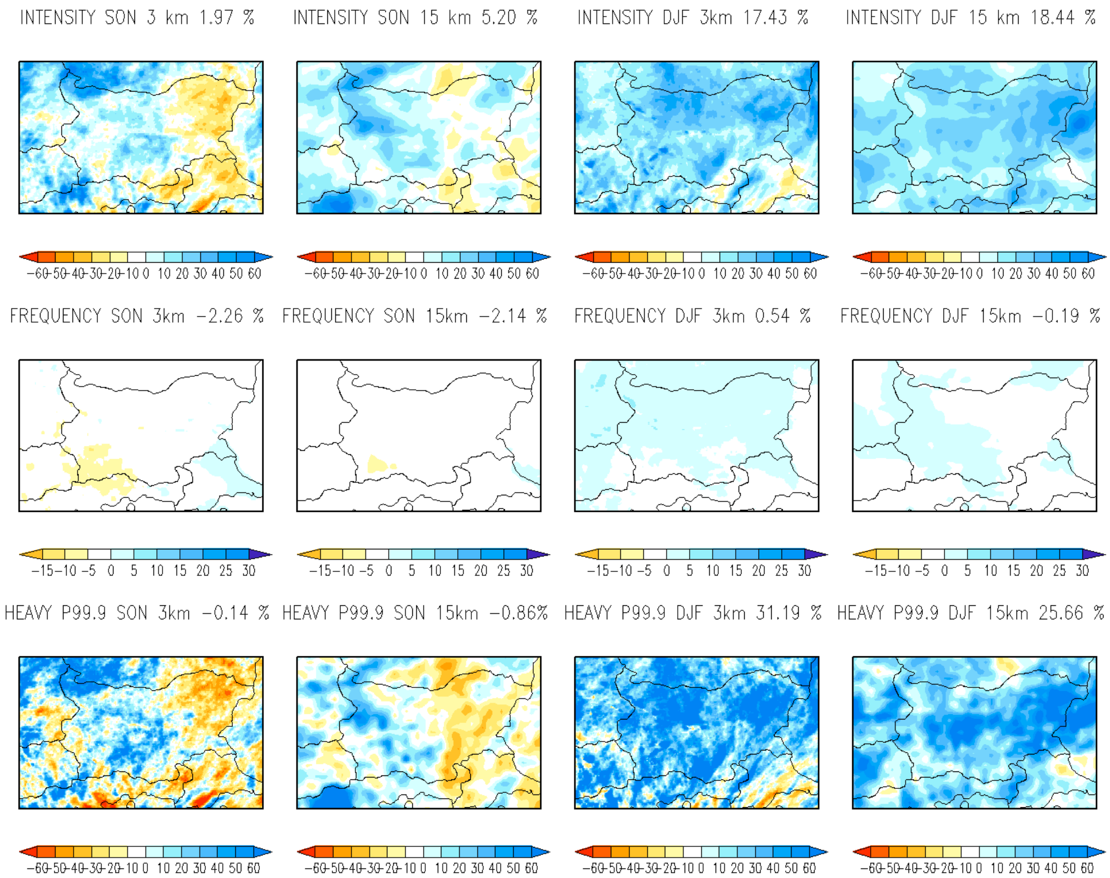

Figure 7. Same as Figure 6, but for the autumn (SON) and winter (DJF).

Table 4. Percentage changes (%) for the two simulations (3 km CPRCM and 15 km RCM) in the analyzed indices for MAM, JJA, SON, and DJF area-averaged for Bulgaria (Figure 1b) for the end of the century 2089–2098 concerning the historical period 1995–2004.

2089–2098	3 km	15 km	3 km	15 km	3 km	15 km	3 km	15 km
	MAM		JJA		SON		DJF	
Hourly								
Mean	−1.93	+2.60	−30.12	−31.92	−17.01	−19.78	+19.49	+13.96
INT	+13.86	+18.11	+17.48	+9.76	+1.97	+5.2	+17.43	+18.44
FREQ	−1.75	−1.21	−2.99	−2.65	−2.26	−2.14	+0.54	−0.19
P99.9	+13.14	+8.71	−15.52	−4.88	−0.14	−0.86	+31.19	+25.66
Daily								
Mean	−1.99	+3.03	−29.44	−31.70	−17.35	−20.00	+19.42	+13.42
INT	+11.12	+13.37	+13.34	+7.53	3.94	+7.15	+22.64	+1.11
FREQ	−4.22	−2.76	−10.17	−11.53	−6.10	−6.35	−0.45	−1.84
P99	+10.84	+12.71	−11.22	−13.88	−2.55	−0.45	+35.30	+30.20

3.2.2. Daily Projection Precipitation Change in 2089−2098 vs. 1995–2004

Figures S8 and S9 in the Supplementary Materials show results for the expected daily precipitation metrics' projected changes. Figure S8 compares expected changes between resolutions in daily mean precipitation, intensity, frequency, and p99 for the spring (first two columns) and summer (last two columns). Figure S9 shows the same values as Figure S8 but for the autumn (SON) and winter (DJF).

Simulated with a 3 km CPRCM, the area-averaged (Table 4) mean daily precipitation is expected to decrease in all seasons (−1.99% in MAM; −29.44% in JJA; −17.35% in SON), except for DJF (+19.42%), and over eastern Bulgaria in the spring (+10), and the north-westernmost parts of Bulgaria in the fall (+10%) (Figures S5 and S6, first row). The intensity of wet days is expected to increase in all seasons (+11.12% in MAM, +13.34% in JJA, +3.94% in SON, and +22.6% in DJF), except in northeastern parts of Bulgaria (the Dobrudzha region) in the fall (Figure S6, second row). The frequency of wet days decreases in all seasons (−4.22% in MAM; −10.17% in JJA; −6.10% in SON; −0.45% in DJF), except over the mountains in the winter (from +5% to +10%) (Figure S6, third row). Heavy precipitation (p99) increases in the spring and winter (+10.84% in MAM and +35.3% in DJF) and decreases in the summer and fall (−11.22% in JJA and −2.55% in SON), except over central (+20%) and northwestern Bulgaria (+30%) in the autumn (Figures S8 and S9, last row).

Simulated with a 15 km RCM, the area−average daily mean precipitation is expected to increase in MAM and DJF (3.03% in MAM; 13.42% in DJF), except in the north-westernmost and south-westernmost parts of Bulgaria in the spring (−20%) (Figure S8, first row). The mean precipitation is expected to decrease in JJA and SON (−31.70% in JJA; −20.0% in SON), except in the north-westernmost parts of Bulgaria in the fall (+10%) (Figures S8 and S9, first row). The wet-day intensity increases in all seasons (13.4% in spring; 7.5% in summer; 7.1% in autumn; and 1.1% in winter). The wet-day frequency is expected to decrease in all seasons (−2.8% in MAM; −11.5% in JJA; −6.4% in SON; −1.8% in DJF), especially in the summer (Figure S8, third row). Heavy precipitation (p99) increases in MAM and DJF (12.7% in MAM; 30.2% in DJF) and decreases in JJA and SON (−13.9% in JJA; −0.5% in SON), except in the central and northwestern parts of Bulgaria in the fall (from +20% to +30%) (Figure S9, last row).

The main differences between the 3 km CPRCM and 15 km RCM projections are shown in the winter wet-day intensity and frequency (Figure S9, second and third row). CPRCM suggests a 22.6% increase in winter wet-day intensity compared with a 1% increase in the 15 km RCM. The km-scale simulation also shows a 5−10% increase in wet-day frequency over the mountains. Both models show an increase in winter heavy precipitation (p99) above 30% by the end of the century. The km-scale simulation also shows an increase in wet-day intensity and p99 in the north-westernmost parts of the county in the autumn (+30%) and decreases in wet-day intensity and p99 over the northeastern parts; the last is not shown in the RCM simulation.

For the precipitation projections, we also compared the results with the driving GCM (HadGEM2-ES) simulation. Figure S10 shows the expected changes in mean daily precipitation, intensity, frequency, and heavy rainfall (p99) using the driving GCM HadGEM2-ES according to the RCP8.5 scenario. Daily mean precipitation is expected to decrease in the summer (−48.19%) and fall (−30.25%) and increase in the winter (+26.22%) and spring (+10% over eastern Bulgaria). The wet-day intensity increases in all seasons (+18.51% in MAM, +27.68% in DJF, and +7.49 in SON), except for the summer (−6.74%). The wet-day frequency decreases in all seasons, except for the winter. Heavy precipitation (p99) is expected to increase in all seasons (+24.33% in the spring, +30.76% in the winter, and +7.33% in the fall), except for the summer (−30.31%).

3.2.3. Mean and Projected Winter (DJF) Snowfall in 2089–2098 vs. 1995–2004

The increase in precipitation intensity and heavy precipitation in the winter (Figure 7) leads to the important question about future changes in snowfall. The 3 km historical climate simulation of the mean winter (December–January–February) snow water equivalent and the projected changes are shown in Figure 8 in cm. There are significant decreases (50−70%) in snowfall over the Bulgarian lowlands (Figure 8b) and a decrease over the main ski resorts in the southwestern part of the country. There is an increase in snowfall only over the highest peaks (above 2000 m elevation) in southwestern (the Rila and the Pirin Mountains) and central Bulgaria (the Balkan Mountains) by 30–40%. The amount of snowfall in the analysis area is expected to decrease significantly by the end of the century. The winter-projected 2 m temperature is expected to increase in this region by 3.5−4 degrees Celsius by the end of the century (Figure 9b). Large changes in winter snowfall can have large consequences for socioeconomic impacts, regional climate feedback, and others.

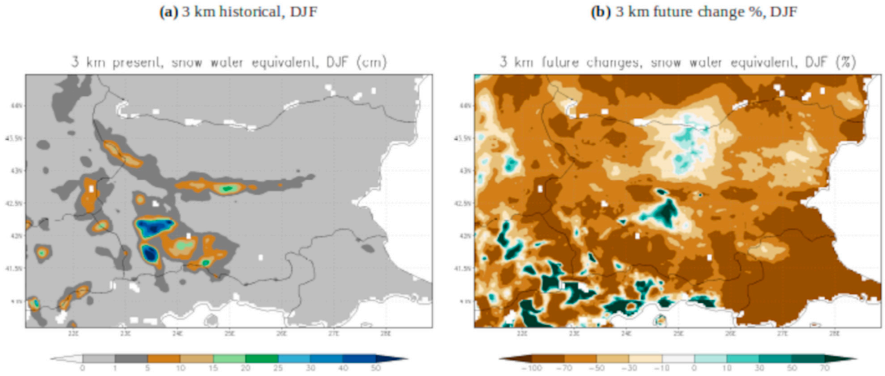

Figure 8. The 3 km historical climate simulation of the DJF snow water equivalent in cm for the period 1995–2004 (**a**) and its 3 km projected future (%) change for 2098–2098 (**b**).

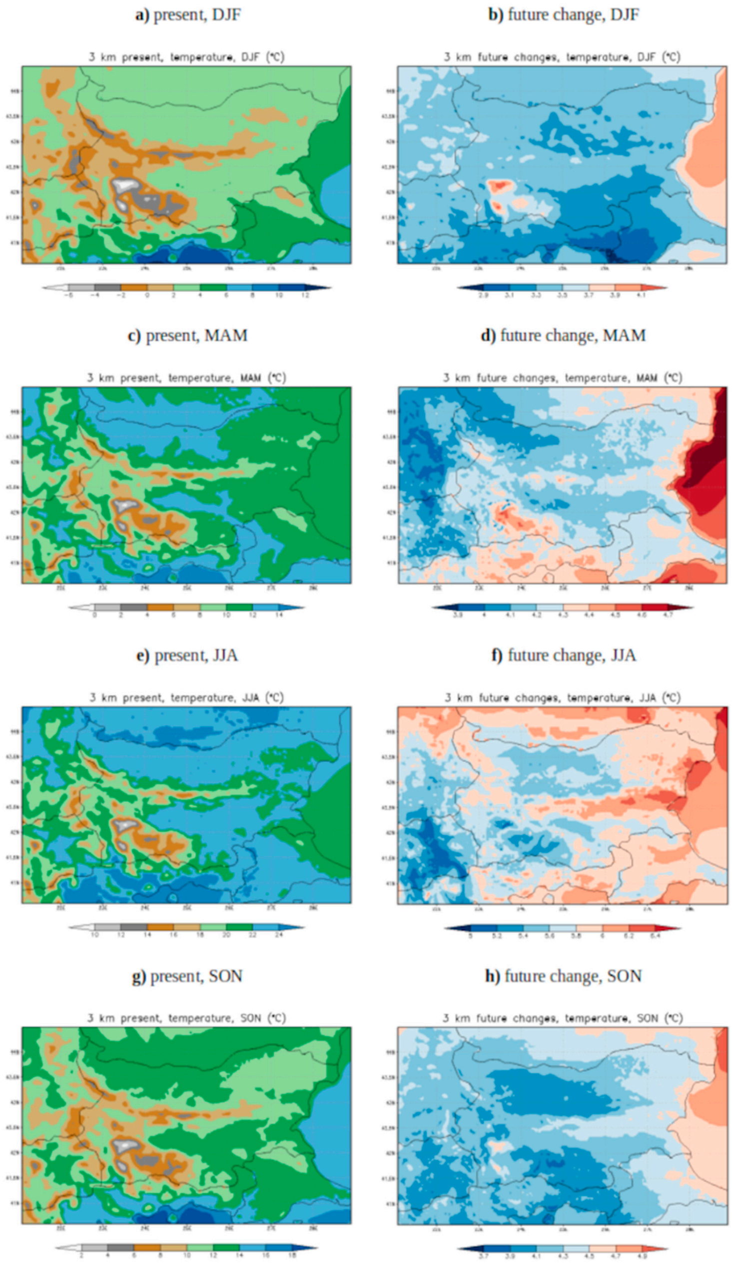

Figure 9. Seasonal mean and projected 2 m temperature simulated with the 3 km CP model (°C) for DJF (**a**,**b**), MAM (**c**,**d**), JJA (**e**,**f**), and SON (**g**,**h**), respectively.

3.2.4. Mean and Projected Seasonal Mean 2 m Temperature in 2089–2098 vs. 1995–2004

The seasonal mean and projected two-meter temperatures are shown in Figure 9 at a grid spacing of 3 km. The average winter temperature (Figure 9a,b) is expected to rise by the end of the century by 3–3.5 °C in the lowlands and by above 4 °C in the mountains. An increase in the 2 m temperature can be expected in all seasons (3.7–4.9 °C in SON, 5–6.4 °C in JJA, 3.9–4.7 °C in MAM, and 2.9–4.1 °C in DJF). The main difference between the 15 km RCM and the 3 km CPRCM (not shown here) simulations is that the km-scale simulation implies a 0.5 °C larger increase in the 2 m temperature over the topography in the spring, autumn, and winter seasons by the end of the century. The increase in temperature is projected to be larger during JJA and MAM (Figure 9d,f), and the warming is projected to be more intense at the topography in all seasons (Figure 9b,d,f,h).

4. Discussion

In this article, we analyzed, for the first time, 3 km RegCM4 convection-permitting model (CPM) projections for Bulgaria. These new simulations allow us to examine the benefits of using CPM across the county. This is the first time CPM has been used to provide Bulgarian future climate projections at the km-scale. This article aimed to produce high spatial and temporal resolution climate change simulations using a convective-permitting model, focused on future precipitation metrics, 2 m temperature, and winter snowfall. The CP simulation is driven by a coarse resolution RCM with a 15 km grid spacing, which, on the other hand, is driven by CMIP5 GCM. The benefits of such high resolution confirm the findings described in [1,6,11,24] for climate and climate changes from the regional to local scale and extreme precipitation.

The results show a better representation of the km-scale simulation compared with the 15 km simulation for hourly precipitation statistics. For wet-hour intensity, we found improvements in CP simulation in all seasons. The improvements were also found for wet-hour frequency in the spring and winter and for heavy precipitation (p99.9) in the autumn and winter. The results are in agreement with [51], where improvements in CP simulations for extreme precipitation were found over Germany using the COSMO-CLM model, and are also in agreement with the ensemble multi-model study over the Alps [11], where the authors show that km-scale models reproduce precipitation metrics more realistically and improve the representation of extreme precipitation.

We also found that on daily and hourly time scales, extreme rainfall is projected to become more intense and less frequent over some areas, especially in the spring and winter, but also in some parts in the fall. The results are consistent with a previous study using the CP model at a 2.2 km grid resolution over the Alps [52]. A widespread decrease (50–70%) in winter snowfall was found across the Bulgarian lowlands and a decrease over the main ski resorts in the southwestern parts of the country. We also found an increase in winter snowfall over the highest peaks only (above 2000 m) (30–40%). We found an increase in winter mean precipitation and extreme rainfall by the end of the century in all simulations (GCM, RCM, CPRCM). The results are consistent with [31], where the authors investigated the Mediterranean influence on the climatic regime over the Balkan Peninsula and found a periodicity of about 20 years, suggesting that the next decade will be characterized by a peak of Mediterranean influence, which means more intense winter precipitation and a relatively colder winter.

An increase in the mean 2-meter temperature in all seasons can be expected. The main difference between RCM and CPRCM is that the kilometer-scale simulation shows 0.5 °C more temperature increases over topography in the spring, fall, and winter. The temperature increase is larger during JJA and MAM. The warming is projected to become more intense at topography in all seasons. The findings are in agreement with a previous study [53]. Comparing GCM, RCM, and CPRCM climate projections, we found that the area-averaged changes in CPRCM and RCM are smaller than GCM, except for the summer intensity, but CPRCM shows larger changes over some regions. All models show an increase in winter precipitation, but CPRCM shows a larger increase in the northeastern and northwestern parts of the country and also over the mountains. In the autumn, the models (GCM, RCM, and CPRCM) show different signals for Bulgaria over some areas. Comparing CPRCM and RCM, we found sign changes in the summer, spring, and fall in daily and hourly heavy precipitation and in daily intensity and in fall hourly intensity over some regions. Overall, the frequency of wet-day and wet-hour precipitation is projected to decrease over Bulgaria, except in the winter, and the intensity increases. Heavy precipitation becomes more intense at both the hourly and daily time scales. These results confirm findings in previous studies over other European domains [18,24]. The reasons for the differences between models are not only the resolution but also the representation of the deep convection processes, which are parametrized in RCM and GCM simulations using the cumulus convection schemes and explicitly resolved with the CPRCM simulation [6].

5. Conclusions

This paper presents the first 10-year-long historical (1995–2004) and future (2089–2098) scenario simulations at a convection-permitting scale (3 km) for the territory of Bulgaria. The main aim of this study is to assess different precipitation metrics and their future projections for Bulgaria under the RCP8.5 scenario. The projected mean 2 m temperature and winter snow water equivalent at a kilometer-scale grid spacing are also presented. The method downscales the HadGEM2-ES global climate model to 15 km grid spacing using the convection-parametrized regional climate model RegCM4.7.1 and after that, downscales to the kilometer-scale (3 km) grid spacing using the convection-permitting model. In addition to resolution, the main difference between the two models is the representation of deep convective processes, which are explicitly resolved with the convection-permitting model and parameterized with a cumulus convective scheme using the RCM model.

The performance of the historical period is assessed against high-resolution datasets and also against the coarse-resolution RCM. The added value of CP simulation mainly derives from a reduction in biases for some precipitation indices, especially at the hourly scale, and a better representation of the fine-scale details of the precipitation distribution. The km-scale simulation presents smaller biases compared with the coarse-resolution simulation for wet-hour intensity (−12% vs. −36.8% in the spring, +3.7% vs. −41.4% in the summer, −44.5% vs. −53.7% in the fall, and −47.6% vs. −57.9% in the winter, respectively), for wet-hour frequency in the spring (−2% vs. −5%) and winter (−5.74% vs. −9.39%), and for heavy precipitation (p99.9) in the autumn (+21.9% vs. −45.7%) and winter (−10.8% vs. −50.3%).

The analysis of the projected changes in rainfall reveals a decrease in the mean summer and autumn precipitation (except the north-westernmost parts of Bulgaria in the fall) and an increase in the mean spring and winter precipitation. The mean and heavy precipitation increase in the spring, becoming less frequent and more intense by the end of the century. In the winter, the mean precipitation increases over the studied domain (15–20%), and heavy precipitation significantly increases (30−35%) over Bulgaria and becomes more intense. In the kilometer-scale experiment, a positive projected change in the wet-hour intensity is expected in all seasons for Bulgaria (13.86% in MAM, 17.48% in JJA, 1.97% in SON, and 17.43% in DJF) and in heavy precipitation (p99.9) in the spring (13.14%) and winter (31.19%). Extreme precipitation (p99) is expected to increase in the winter (+35.3%) and spring (+10.84%) for both resolutions for the territory of Bulgaria by the end of the century. An increase in the mean 2-meter temperature in all seasons can be expected between 3.7 and 4.9 °C in the fall, 5 and 6.4 °C in the summer, 3.9 and 4.7 °C in the spring, and 2.9 and 4.1 °C in the winter. The warming becomes more intense at the topography in all seasons, especially in the winter. The amount of snow in the analysis area decreases significantly by the end of the century. A decrease in winter snowfall is found across the country (50–70%), except in the highest elevation peaks (30–40%).

The results provide a basis for further investigations and data for the scale gap between regional climate models and impact models used in hydrology and agrometeorology. The novel aspects of this article relate to producing very high spatial and temporal resolution climate change information for the territory of Bulgaria that will be of interest to climate information users, such as policymakers, stakeholders, and others, for the evaluation of the added value of CPM simulation regarding RCM simulation and the assessment of the impact of climate change on different precipitation metrics, winter snowfall, and 2 m temperature for Bulgaria.

Supplementary Materials: The following supporting information can be downloaded at: https://www.mdpi.com/article/10.3390/atmos15010091/s1, Figure S1. Spatial distribution of seasonal mean daily precipitation (mm/d) from observations (MESCAN-SURFEX) and simulations (3 km CPRCM and 15 km RCM) (first three columns) and mean biases of CPRCM and RCM with respect to MESCAN-SURFEX (last two columns) for the spring—MAM (first row), summer—JJA (second row), autumn—SON (third row) and winter—DJF (last row). The simulated historical period is 1995–2004; Figure S2. Spatial distribution of seasonal mean wet-day intensity (> 1 mm/d) in mm/d from observations (MESCAN-SURFEX) and simulations (3 km CPRCM and 15 km RCM) (first three columns) and mean biases of CPRCM and RCM with respect to MESCAN-SURFEX (last two columns) for the spring—MAM (first row), summer—JJA (second row), autumn—SON (third row) and winter—DJF (last row). The simulated historical period is 1995–2004; Figure S3. Spatial distribution of wet-day frequency (>1 mm/d) in % from observations (MESCAN-SURFEX) and simulations (3 km CPRCM and 15 km RCM) (first three columns) and mean biases of CPRCM and RCM with respect to MESCAN-SURFEX (last two columns) for the spring—MAM (first row), summer—JJA (second row), autumn—SON (third row) and winter—DJF (last row). The simulated historical period is 1995–2004; Figure S4. Spatial distribution of heavy precipitation (p99) in mm/d from observations (MESCAN-SURFEX) and simulations (3 km CPRCM and 15 km RCM) (first three columns) and mean biases of CPRCM and RCM with respect to MESCAN-SURFEX (last two columns) for the spring—MAM (first row), summer—JJA (second row), autumn—SON (third row) and winter—DJF (last row). The simulated historical period is 1995–2004; Figure S5. Spatial distribution of seasonal mean biases in the CPRCM simulation (3 km) with respect to the daily PDIR-Now dataset for mean daily precipitation in mm/d (first row), precipitation intensity (mm/d) (second row), frequency (%), and heavy precipitation (p99) in mm/d (last row) for the spring—MAM, summer—JJA, autumn—SON, and winter—DJF. The simulated historical period is 2001–2004. The area-average biases are on the top of each image; Figure S6. Spatial distribution of seasonal mean biases in the RCM simulation (15 km) with respect to the daily PDIR-Now dataset for mean daily precipitation in mm/d (first row), precipitation intensity (mm/d) (second row), frequency (%), and heavy precipitation (p99) in mm/d (last row) for the spring—MAM, summer—JJA, autumn—SON, and winter—DJF. The simulated historical period is 2001–2004. The area-average biases are on the top of each image; Figure S7. Probability density function (PDF) for the daily precipitation in Bulgaria from simulations (CPRCM and RCM) and observations (PDIR-Now and MESCAN-SURFEX) for the historical (1995–2004) and future periods (2089–2098). PDIR-Now is available for the period 2001–2004; Figure S8. Expected changes in daily precipitation (first row), intensity (second row), frequency (third row), and heavy precipitation (p99) (last row) from both models (3 km CPRCM and 15km RCM) related to the spring—MAM (first two columns, respectively) and summer—JJA (last two columns, respectively) projected at the end of the century (2089–2098) with respect to the historical period (1995–2004) in %; Figure S9. Expected changes in daily precipitation (first row), intensity (second row), frequency (third row), and heavy precipitation (p99) (last row) from both models (3 km CPRCM and 15km RCM) related to the fall—SON (first two columns, respectively) and winter—DJF (last two columns, respectively) projected at the end of the century (2089–2098) with respect to the historical period (1995–2004) in %; Figure S10. Expected changes in mean daily precipitation (first row), precipitation intensity (second row), frequency (third row), and heavy rainfall (p99) (last row) from driving GCM HadGEM2-ES according to the RCP8.5 scenario related to the spring—MAM (first column), summer—JJA (second columns), fall—SON (third column), and winter—DJF (last column) projected at the end of the century (2089–2098) concerning the historical period (1995–2004) in %.

Author Contributions: Conceptualization, R.V. and N.G.; methodology, R.V. and I.P.; software, R.V.; validation, R.V., I.P., and N.G.; formal analysis, R.V.; investigation, R.V.; resources, R.V., N.G., and I.P.; data curation, R.V., N.G., and I.P.; writing—original draft preparation, R.V.; writing—review and editing, R.V.; visualization, N.G., I.P., and R.V.; project administration, R.V.; funding acquisition, R.V., I.P., and N.G. All authors have read and agreed to the published version of the manuscript.

Funding: This research was funded by the Bulgarian National Science Fund, grant number KP−06−M57/3.

Institutional Review Board Statement: Not applicable.

Informed Consent Statement: Not applicable.

Data Availability Statement: The data and methods used in this research are presented in sufficient detail in this article. In this study, we used publicly archived high-resolution datasets available at the following links: UERRA MESCAN−SURFEX data, https://cds.climate.copernicus.eu/cdsapp#!/dataset/reanalysis%E2%88%92uerra%E2%88%92europe%E2%88%92single%E2%88%92levels?tab=overview, accessed on 30 May 2023, and PDIR−Now data, https://chrsdata.eng.uci.edu/, accessed on 16 May 2023.

Acknowledgments: We acknowledge Discoverer PetaSC and EuroHPC JU for awarding this project access to Discoverer supercomputer resources. The authors acknowledge the Center for Hydrometeorology and Remote Sensing (CHRS) at the University of California, Irvine (UCI), for providing the PERSIANN Dynamic Infrared–Rain Rate (PERSIANN−PDIR−Now) dataset (accessed on 16 May 2023). The authors acknowledge the Copernicus Climate Change Service and Climate Data Store. The simulations were performed with the non-hydrostatic RegCM model. The RegCM model code is available at https://doi.org/10.5281/zenodo.4603556 (accessed on 23 December 2021). We thank the Earth System Physics group at the ICTP for providing free-of-charge RegCM software. The authors would like to thank the anonymous reviewers for their efforts, comments, and suggestions, which helped us improve the quality of this manuscript.

Conflicts of Interest: The authors declare no conflicts of interest.

References

1. Coppola, E.; Sobolowski, S.; Pichelli, E.; Raffaele, F.; Ahrens, B.; Anders, I.; Ban, N.; Bastin, S.; Belda, M.; Belusic, D.; et al. A first-of-its-kind multi-model convection permitting ensemble for investigating convective phenomena over Europe and the Mediterranean. *Clim. Dyn.* **2020**, *55*, 3–34. [CrossRef]
2. Coppola, E.; Stocchi, P.; Pichelli, E.; Alavez, J.A.T.; Glazer, R.; Giuliani, G.; Di Sante, F.; Nogherotto, R.; Giorgi, F. Non-Hydrostatic RegCM4 (RegCM4-NH): Model description and case studies over multiple domains. *Geosci. Model Dev.* **2021**, *14*, 7705–7723. [CrossRef]
3. Lucas-Picher, P.; Argüeso, D.; Brisson, E.; Tramblay, Y.; Berg, P.; Lemonsu, A.; Kotlarski, S.; Caillaud, C. Convection-permitting modeling with regional climate models: Latest developments and next steps. In *Wiley Interdisciplinary Reviews: Climate Change*; Wiley Online Library: Hoboken, NJ, USA, 2021; Volume 12, p. e731.
4. Kendon, E.J.; Ban, N.; Roberts, N.M.; Fowler, H.J.; Roberts, M.J.; Chan, S.C.; Evans, J.P.; Fosser, G.; Wilkinson, J.M. Do convection-permitting regional climate models improve projections of future precipitation change? *Bull. Am. Meteorol. Soc.* **2017**, *98*, 79–93. [CrossRef]
5. Kendon, E.J.; Prein, A.F.; Senior, C.A.; Stirling, A. Challenges and outlook for convection-permitting climate modelling. *Philos. Trans. R. Soc. A* **2021**, *379*, 20190547. [CrossRef]
6. Prein, A.F.; Langhans, W.; Fosser, G.; Ferrone, A.; Ban, N.; Goergen, K.; Keller, M.; Tölle, M.; Gutjahr, O.; Feser, F.; et al. A review on regional convection-permitting climate modeling: Demonstrations, prospects, and challenges. *Rev. Geophys.* **2015**, *53*, 323–361. [CrossRef] [PubMed]
7. Kendon, E.J.; Roberts, N.M.; Senior, C.A.; Roberts, M.J. Realism of Rainfall in a Very High-Resolution Regional Climate Model. *J. Clim.* **2012**, *25*, 5791–5806. [CrossRef]
8. Déqué, M.; Rowell, D.P.; Lüthi, D.; Giorgi, F.; Christensen, J.H.; Rockel, B.; Jacob, D.; Kjellström, E.; de Castro, M.; Hurk, B.v.D. An intercomparison of regional climate simulations for Europe: Assessing uncertainties in model projections. *Clim. Chang.* **2007**, *81*, 53–70. [CrossRef]
9. Ban, N.; Schmidli, J.; Schär, C. Evaluation of the convection-resolving regional climate modeling approach in decade-long simulations. *J. Geophys. Res. Atmos.* **2014**, *119*, 7889–7907. [CrossRef]
10. Hewitt, C.D.; Lowe, J.A. Toward a European Climate Prediction System. *Bull. Am. Meteorol. Soc.* **2018**, *99*, 1997–2001. [CrossRef]
11. Ban, N.; Caillaud, C.; Coppola, E.; Pichelli, E.; Sobolowski, S.; Adinolfi, M.; Ahrens, B.; Alias, A.; Anders, I.; Bastin, S.; et al. The first multi-model ensemble of regional climate simulations at the kilometer-scale resolution, part I: Evaluation of precipitation. *Clim. Dyn.* **2021**, *57*, 275–302. [CrossRef]
12. Stocchi, P.; Pichelli, E.; Alavez, J.A.T.; Coppola, E.; Giuliani, G.; Giorgi, F. Non-Hydrostatic Regcm4 (Regcm4-NH): Evaluation of Precipitation Statistics at the Convection-Permitting Scale over Different Domains. *Atmosphere* **2022**, *13*, 861. [CrossRef]
13. Prein, A.F.; Gobiet, A.; Suklitsch, M.; Truhetz, H.; Awan, N.K.; Keuler, K.; Georgievski, G. Added value of vonvection permitting seasonal simulations. *Clim. Dyn.* **2013**, *41*, 2655–2677. [CrossRef]

14. Lucas-Picher, P.; Brisson, E.; Caillaud, C.; Alias, A.; Nabat, P.; Lemonsu, A.; Poncet, N.; Hernandez, V.E.C.; Michau, Y.; Doury, A.; et al. Evaluation of the convection-permitting regional climate model CNRM-AROME41t1 over Northwestern Europe. *Clim. Dyn.* **2023**. [CrossRef]
15. Chan, S.C.; Kendon, E.J.; Fowler, H.J.; Blenkinsop, S.; Roberts, N.M. Projected increases in summer and winter UK sub-daily precipitation extremes from high-resolution regional climate models. *Environ. Res. Lett.* **2014**, *9*, 084019. [CrossRef]
16. Fosser, G.; Khodayar, S.; Berg, P. Benefit of convection permitting climate model simulations in the representation of convective precipitation. *Clim. Dyn.* **2015**, *44*, 45–60. [CrossRef]
17. Lind, P.; Lindstedt, D.; Kjellström, E.; Jones, C. Spatial and Temporal Characteristics of Summer Precipitation over Central Europe in a Suite of High-Resolution Climate Models. *J. Clim.* **2016**, *29*, 3501–3518. [CrossRef]
18. Adinolfi, M.; Raffa, M.; Reder, A.; Mercogliano, P. Evaluation and Expected Changes of Summer Precipitation at Convection Permitting Scale with COSMO-CLM over Alpine Space. *Atmosphere* **2020**, *12*, 54. [CrossRef]
19. Chan, S.C.; Kendon, E.J.; Berthou, S.; Fosser, G.; Lewis, E.; Fowler, H.J. Europe-wide precipitation projections at convection permitting scale with the Unified Model. *Clim. Dyn.* **2020**, *55*, 409–428. [CrossRef]
20. Berthou, S.; Kendon, E.J.; Chan, S.C.; Ban, N.; Leutwyler, D.; Schär, C.; Fosser, G. Pan-European climate at convection-permitting scale: A model intercomparison study. *Clim. Dyn.* **2018**, *55*, 35–59. [CrossRef]
21. Leutwyler, D.; Lüthi, D.; Ban, N.; Fuhrer, O.; Schär, C. Evaluation of the convection-resolving climate modeling approach on continental scales. *J. Geophys. Res.* **2017**, *122*, 5237–5258. [CrossRef]
22. Kendon, E.J.; Stratton, R.A.; Tucker, S.; Marsham, J.H.; Berthou, S.; Rowell, D.P.; Senior, C.A. Enhanced future changes in wet and dry extremes over Africa at convection-permitting scale. *Nat. Commun.* **2019**, *10*, 1794. [CrossRef]
23. Liu, C.; Ikeda, K.; Rasmussen, R.; Barlage, M.; Newman, A.J.; Prein, A.F.; Yates, D. Continental-scale convection-permitting modeling of the current and future climate of North America. *Clim. Dyn.* **2016**, *49*, 71–95. [CrossRef]
24. Pichelli, E.; Coppola, E.; Sobolowski, S.; Ban, N.; Giorgi, F.; Stocchi, P.; Alias, A.; Belušić, D.; Berthou, S.; Caillaud, C.; et al. The first multi-model ensemble of regional climate simulations at kilometer-scale resolution part 2: Historical and future simulations of precipitation. *Clim. Dyn.* **2021**, *56*, 3581–3602. [CrossRef]
25. Hodnebrog, Ø.; Marelle, L.; Alterskjær, K.; Wood, R.R.; Ludwig, R.; Fischer, E.M.; Richardson, T.B.; Forster, P.M.; Sillmann, J.; Myhre, G. Intensification of summer precipitation with shorter time-scales in Europe. *Environ. Res. Lett.* **2019**, *14*, 124050. [CrossRef]
26. Prein, A.F.; Rasmussen, R.; Castro, C.L.; Dai, A.; Minder, J. Special issue: Advances in convection-permitting climate modeling. *Clim. Dyn.* **2020**, *55*, 1–2. [CrossRef]
27. Giorgi, F.; Coppola, E.; Solmon, F.; Mariotti, L.; Sylla, M.B.; Bi, X.; Elguindi, N.; Diro, G.T.; Nair, V.; Giuliani, G.; et al. RegCM4: Model description and preliminary tests over multiple CORDEX domains. *Clim. Res.* **2012**, *52*, 7–29. [CrossRef]
28. Valcheva, R.; Popov, I.; Gerganov, N. Convection-Permitting Regional Climate Simulation over Bulgaria: Assessment of Precipitation Statistics. *Atmosphere* **2023**, *14*, 1249. [CrossRef]
29. Valcheva, R.; Popov, I.; Gerganov, N. Assessment of precipitation statistics with non-hydrostatic regional climate model RegCM4.7.1 at regional and convection-permitting scale over Bulgaria. In Proceedings of the EGU General Assembly 2023, Vienna, Austria, 24–28 April 2023. EGU23-9768. [CrossRef]
30. Valcheva, R.; Spiridonov, V. Regional climate projections of heavy precipitation over the Balkan Peninsula. *IDŐJÁRÁS Q. J. Hung. Meteorol. Serv.* **2023**, *127*, 77–106. [CrossRef]
31. Peneva, E.; Matov, M.; Tsekov, M. Mediterranean Influence on the Climatic Regime over the Balkan Peninsula from 1901–2021. *Climate* **2023**, *11*, 68. [CrossRef]
32. Kiehl, J.; Hack, J.; Bonan, G.; Boville, B.; Briegleb, B.; Williamson, D.; Rasch, P. *Description of the NCAR Community Climate Model (CCM3)*; NCAR Tech. Note; National Center for Atmospheric Research: Boulder, CO, USA, 1996; Volume NCAR/TN-420+STR, 159p.
33. Holtslag, A.A.M.; De Bruijn, E.I.F.; Pan, H.-L. A high resolution air mass transformation model for short-range weather forecasting. *Mon. Weather. Rev.* **1990**, *118*, 1561–1575. [CrossRef]
34. Pal, J.S.; Small, E.E.; Eltahir, E.A.B. Simulation of regional-scale water and energy budgets: Representation of subgrid cloud and precipitation processes within RegCM. *J. Geophys. Res. Atmos.* **2000**, *105*, 29579–29594. [CrossRef]
35. Dickinson, R.; Henderson-Sellers, A.; Kennedy, P. *Biosphere–Atmosphere Transfer Scheme (BATS) Version 1e as Coupled to the NCAR Community Climate Model*; TechRep; National Center for Atmospheric Research: Boulder, CO, USA, 1993; Volume NCAR/TN-387+STR, 80p.
36. Zeng, X.; Zhao, M.; Dickinson, R.E. Intercomparison of bulk aerodynamic algorithms for the computation of sea surface fluxes using TOGA COARE and TAO data. *J. Clim.* **1998**, *11*, 2628–2644. [CrossRef]
37. Kain, J.S.; Fritsch, J.M. A one-dimensional entraining/detraining plume model and its application in convective parameterization. *J. Atmos. Sci.* **1990**, *47*, 2784–2802. [CrossRef]
38. Kain, J.S. The Kain–Fritsch convective parameterization: An update. *J. Appl. Meteor.* **2004**, *43*, 170–181. [CrossRef]
39. Grell, G.A.; Dudhia, J.; Stauffer, D.R. *A Description of the Fifth-Generation Penn State/NCAR Mesoscale Model (MM5)*; NCAR Tech Note NCAR/TN-398 + STR; NCAR: Boulder, CO, USA, 1994.

40. Valcheva, R.; Popov, I.; Gerganov, N. A sensitivity study of the non-hydrostatic regional climate model RegCM-4.7.1 to physical parametrization schemes over the Balkan peninsula and Bulgaria, International Multidisciplinary Scientific GeoConference Surveying Geology and Mining Ecology Management. *SGEM* **2022**, *22*, 159–168.
41. Collins, W.J.; Bellouin, N.; Doutriaux-Boucher, M.; Gedney, N.; Halloran, P.; Hinton, T.; Hughes, J.; Jones, C.D.; Joshi, M.; Liddicoat, S.; et al. Development and evaluation of an Earth-System model—HadGEM2. *Geosci. Model Dev.* **2011**, *4*, 1051–1075. [CrossRef]
42. Riahi, K.; Grübler, A.; Nakicenovic, N. Scenarios of long-term socio-economic and environmental development under climate stabilization. *Technol. Forecast. Soc. Chang.* **2007**, *74*, 887–935. [CrossRef]
43. Bazile, E.; Abida, R.; Verelle, A.; Le Moigne, P.; Szczypta, C. MESCAN-SURFEX Surface Analysis, Deliverable D2.8 of the UERRA Project. 2017. Available online: http://www.uerra.eu/publications/deliverable-reports.html (accessed on 30 May 2023).
44. Soci, C.; Bazile, E.; Besson, F.; Landelius, T. High-resolution precipitation re-analysis system for climatological purposes. *Tellus A Dyn. Meteorol. Oceanogr.* **2016**, *68*, 29879. [CrossRef]
45. Nguyen, P.; Ombadi, M.; Gorooh, V.A.; Shearer, E.J.; Sadeghi, M.; Sorooshian, S.; Hsu, K.; Bolvin, D.; Ralph, M.F. PERSIANN Dynamic Infrared-Rain Rate (PDIR-Now): A Near-real time, Quasi-Global Satellite Precipitation Dataset. *J. Hydrometeorol.* **2020**, *21*, 2893–2906. [CrossRef]
46. Prein, A.F.; Gobiet, A. Impacts of uncertainties in European gridded precipitation observations on regional climate analysis. *Int. J. Clim.* **2017**, *37*, 305–327. [CrossRef]
47. Bartsotas, N.S.; Anagnostou, E.N.; Nikolopoulos, E.I.; Kallos, G. Investigating Satellite Precipitation Uncertainty over Complex Terrain. *J. Geophys. Res. Atmos.* **2018**, *123*, 5346–5359. [CrossRef]
48. Sarachi, S.; Hsu, K.-L.; Sorooshian, S. A Statistical Model for the Uncertainty Analysis of Satellite Precipitation Products. *J. Hydrometeorol.* **2015**, *16*, 2101–2117. [CrossRef]
49. Tian, Y.; Peters-Lidard, C.D. A global map of uncertainties in satellite-based precipitation measurements. *Geophys. Res. Lett.* **2010**, *37*. [CrossRef]
50. Schär, C.; Ban, N.; Fischer, E.M.; Rajczak, J.; Schmidli, J.; Frei, C.; O'Gorman, P.A. Percentile indices for assessing changes in heavy precipitation events. *Clim. Chang.* **2016**, *137*, 201–216. [CrossRef]
51. Rybka, H.; Haller, M.; Brienen, S.; Brauch, J.; Früh, B.; Junghänel, T.; Lengfeld, K.; Walter, A.; Winterrath, T. Convection-permitting climate simulations with COSMO-CLM for Germany: Analysis of present and future daily and sub-daily extreme precipitation. *Meteorol. Z.* **2023**, *32*, 91–111. [CrossRef]
52. Ban, N.; Schmidli, J.; Schär, C. Heavy precipitation in a changing climate: Does short-term summer precipitation increase faster? *Geophys. Res. Lett.* **2015**, *42*, 1165–1172. [CrossRef]
53. Lüthi, S.; Ban, N.; Kotlarski, S.; Steger, C.R.; Jonas, T.; Schär, C. Projections of Alpine Snow-Cover in a High-Resolution Climate Simulation. *Atmosphere* **2019**, *10*, 463. [CrossRef]